

Robustness of quantum memories based on Majorana zero modes

L. Mazza,^{1,2,*} M. Rizzi,¹ M. D. Lukin,³ and J. I. Cirac¹

¹*Max-Planck-Institut für Quantenoptik, Hans-Kopfermann-Strasse 1, D-85748 Garching, Germany*

²*Scuola Normale Superiore, piazza dei Cavalieri 7, I-56127, Pisa, Italy*

³*Physics Department, Harvard University, Cambridge, Massachusetts 02138, USA*

We analyze the robustness of a quantum memory based on Majorana modes in a Kitaev chain. We identify the optimal recovery operation acting on the memory in the presence of perturbations and evaluate its fidelity in different scenarios. We show that for time-dependent Hamiltonian perturbations that preserve the topological features, the memory is robust even if the perturbation contains frequencies that lie well above the gap. We identify the condition that is responsible for this feature. At the same time we find that the memory is unstable with respect to particle losses.

Introduction. Quantum memories for the reliable storage of quantum states over long times constitute one of the basic ingredients for most applications in quantum information science [1, 2]. The so-called self-protected quantum memories (SPQM) [3, 4] constitute appealing candidates for realization of quantum memories. Here, the quantum state is stored in the low-energy subspace of a many-body quantum system, and the interactions among its elementary constituents provide the protection against perturbations. As a key feature, active error correction is not required. A single recovery operation at the time of retrieving the quantum state [5] is sufficient. The degree of protection may, however, not be as strong as that offered by fault-tolerant error correction [6]. In recent years, a significant effort has been devoted to quantify the robustness of SPQMs against different types of perturbations [4, 5, 7–14].

Topological superconductors (TSc) hosting spatially-localized zero-energy Majorana modes [15–17] are attractive candidates for a SPQM. Those systems exhibit a gapped quasi-degenerate ground state subspace whose internal energy splitting closes exponentially with the system size of the system, even in presence of small local imperfections [18]. Thus, the dephasing time of a qubit encoded in that subspace grows exponentially with the size of the system. This intriguing property is associated to the topological character of the TSc [15, 18], and thus it is referred to as *topological protection* of the information. Moreover, the fermion parity superselection rule can be used to protect the qubit against flip errors, as long as the environment does not introduce single particles in the system [19]. Although Majorana modes are hard to find in Nature, several proposals to engineer them have been put forward [20, 21]. The experimental observation and study of such modes are now actively being pursued [22].

The robustness of quantum memories based on Majorana modes has been analyzed under two assumptions (see, eg. [12, 19, 23, 24]): (i) the quantum state is stored in the quasi-degenerate ground state of the (eventually) perturbed Hamiltonian [25]; (ii) a particular recovery operation is applied. Whereas those assumptions are justified in some scenarios, this is not always the case. For

instance, in cases when the qubit is not stored in the ground subspace of the Hamiltonian, either because the latter is not known, or it suddenly changes in time, all the eigenstates of the Hamiltonian are involved in the dynamics. Thus the robustness cannot only rely on its ground state properties [26]. Moreover, even if the standard recovery operation fails to retrieve the original state, there may exist more general operations that could accomplish this task. In this case the information about the stored state may still exist in the system, but cannot be extracted with the standard recovery.

In this Letter we study the robustness of a quantum memory based on the Majorana modes of the Kitaev chain [17] to both Hamiltonian perturbations and interactions with the environment. Focusing on the scaling of the memory time with the system size, we first develop the formalism to identify the optimal recovery operation in the presence of perturbations and evaluate the optimal recovery fidelity. We next consider the storage of a qubit in the ground state of a given Hamiltonian, while the evolution takes place according to a different one. We find that, as long as the original and (instantaneous) perturbed Hamiltonians are within the topological phase, the memory time grows exponentially with the system size, even if the perturbation contains frequencies well above the gap. This implies that protection in this dynamical scenario is not only related to the topological character of the ground state of the Hamiltonian, but to a dynamical condition which we identify. Furthermore, this provides us with an example of a memory that is not stable with the standard syndrome-based recovery operation [12, 27], but can still be made robust by carefully choosing a more general operation. We also investigate the effects of temperature, the coupling to a reservoir involving particle exchange, and the restriction to Gaussian recovery operations [28, 29].

Setup. We consider a Kitaev chain of $2N$ Majorana modes, $\{\hat{c}_j\}$, with $\hat{c}_j^\dagger = \hat{c}_j$ and $\{\hat{c}_j, \hat{c}_k\}_+ = 2\delta_{j,k}$. The Hamiltonian is [17]:

$$\hat{H}(\mu) = \frac{iJ}{2} \sum_{j=1}^{N-1} \hat{c}_{2j} \hat{c}_{2j+1} - \frac{i\mu}{2} \sum_{j=1}^N \hat{c}_{2j-1} \hat{c}_{2j}. \quad (1)$$

At zero temperature, it has a topological phase in the regime $|\mu/J| < 2$. There, the ground state is quasi-degenerate due to the existence of (nearly) zero energy Majorana modes, $\hat{m}_{1,2}$ localized at the edges. They can be expressed as linear combinations of the $\{\hat{c}\}$, and define a Dirac mode $\hat{a} = \frac{1}{2}(\hat{m}_1 + i\hat{m}_2)$. Due to superselection rules, we need two such modes to build a qubit, and thus we consider two Kitaev chains, with (Dirac) modes \hat{a} and \hat{b} . We construct a set of Pauli operators:

$$\hat{\sigma}'_x = -(\hat{a}\hat{b} + \hat{b}^\dagger\hat{a}^\dagger); \quad \hat{\sigma}'_y = i(\hat{a}\hat{b} - \hat{b}^\dagger\hat{a}^\dagger); \quad \hat{\sigma}'_z = \hat{1} - \hat{a}^\dagger\hat{a} - \hat{b}^\dagger\hat{b}; \quad (2)$$

and define a qubit in the even parity sector: $\text{span}\{|0\rangle = |\text{vac}\rangle, |1\rangle = \hat{a}^\dagger\hat{b}^\dagger|\text{vac}\rangle\}$ [30].

The chains have non-trivial dynamics and (possibly) interact with the environment. Let us denote by \mathcal{D}_t the *decoherence channel* that describes the time evolution including the action of the *protecting Hamiltonian* (1). It maps the state of the qubit onto the state of the two chains [31]. The chains are kept far apart, so that they do not interact with each other, nor with the same environment. In such a case, we can simplify the analysis by assuming that the second Dirac mode, \hat{b} , does not undergo any dynamics.

Optimal recovery of the information. After the storage time t , we attempt to retrieve the qubit by applying a recovery channel, \mathcal{R}_t , to the chain and the extra fermionic mode, \hat{b} . It maps back $N + 1$ fermionic modes onto the qubit defined in terms of (2). The composite channel $\mathcal{T}_t := \mathcal{R}_t \circ \mathcal{D}_t$ describes the complete action on the qubit. \mathcal{R}_t has to be chosen such that \mathcal{T}_t is as close as possible to the identity channel. This can be quantified with the *recovery fidelity*:

$$F(\mathcal{R}_t) = \int d\mu_\varphi \langle \varphi | \mathcal{T}_t(|\varphi\rangle\langle\varphi|) | \varphi \rangle, \quad (3)$$

where the integral is over the surface of the Bloch sphere.

We find that the optimal fidelity is (see the appendix):

$$F_t^{\text{opt}} = \max_{\mathcal{R}_t} F(\mathcal{R}_t) = \frac{2}{3} + \frac{1}{6} \|\hat{\rho}_+(t) - \hat{\rho}_-(t)\|_{\text{tr}}; \quad (4)$$

where $\hat{\rho}_\pm(t) = \mathcal{D}_t(\hat{\rho}_{q,\pm})$, $\hat{\rho}_{q,\pm} = (\hat{1} \pm \hat{\sigma}'_x)/2$, and $\|\cdot\|_{\text{tr}}$ denotes the trace norm. If we restrict the analysis to Gaussian recovery operations,

$$F_{G,t}^{\text{opt}} = \max_{\mathcal{R}_t \text{ is Gaussian}} F(\mathcal{R}_t) = \frac{2}{3} + \frac{1}{6} \|\Gamma_+(t) - \Gamma_-(t)\|_{\text{op}}. \quad (5)$$

Here, $\Gamma_\pm(t)$ are the $2N \times 2N$ covariance matrices (CM) of $\rho_\pm(t)$ defined as $[\Gamma_\pm]_{j,k} = i\text{tr}[\hat{\rho}_\pm \hat{c}_j \hat{c}_k]$ (see [28]), and $\|\cdot\|_{\text{op}}$ is the operator norm. Note that $F_{G,t}^{\text{opt}}$ provides a lower bound to the optimal recovery fidelity. Expressions (4) and (5) can be understood as follows. Due to the imperfections, the distance between any two orthogonal qubit states decreases with time, and no physical recovery action can increase it again [32]. Thus, the fidelity is

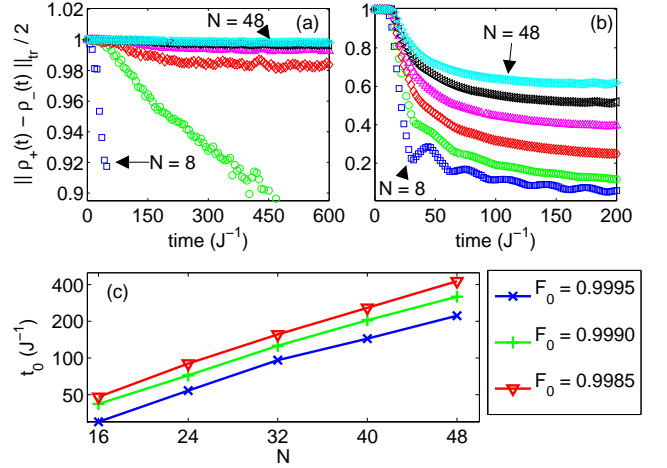


FIG. 1: Robustness of the quantum memory against Hamiltonian perturbations: $\mu_0 = 0$ and: (a,c) $\mu_- = J, \mu_+ = 1.5J$; (b) $\mu_- = 2.5J, \mu_+ = 3J$. Upper panels (a,b): Fidelity as a function of time for different chain lengths, $N = 8, 16, 24, 32, 40$ and 48 . Lower panel (c): Memory time t_0 as function of N for different values of the fidelity threshold F_0 . We considered $N_d = 101$ realizations uniformly distributed in the range $[\mu_-, \mu_+]$. Data show convergence behavior for $N_d \rightarrow \infty$ (see the appendix) and can therefore be considered as an approximation of the continuum situation.

entirely characterized by the distance between the states evolved out of two orthogonal vectors [33]. The recovery operation that reaches the optimal fidelity tries to align back the image of the Bloch sphere and consists of a unitary operation followed by the discarding of all the extra fermionic modes. In the general case, it may involve N -body terms acting on all the fermionic modes of the chain and its specific form depends on the singular value decomposition of $\hat{\rho}_+(t) - \hat{\rho}_-(t)$ (see the appendix for details). In the simpler Gaussian case, the unitary operation is an evolution with a Hamiltonian similar to the original one (see the appendix).

Hamiltonian perturbations. We consider first the effect of perturbations of the Hamiltonian: we assume the perfect encoding of the qubit using the two lowest-energy eigenstates of $\hat{H}_0 = \hat{H}(\mu_0)$, and then we add an unknown perturbation, \hat{V} . Such perturbation is randomly chosen from a set according to some measure $\nu_{\hat{V}}$. We then add incoherently the corresponding evolutions [31]

$$\mathcal{D}_t(\hat{\rho}_q) = \int d\nu_{\hat{V}} e^{-i(\hat{H}_0 + \hat{V})t} \hat{\rho}(0) e^{i(\hat{H}_0 + \hat{V})t}. \quad (6)$$

We choose \hat{V} quadratic in the Majorana operators, so that we can efficiently evolve each term of the integral [34]. F_t^{opt} can be computed by using a discrete measure and taking into account that $\mathcal{D}_t(\hat{\rho}_q)$ has support in a relatively small subspace (see the appendix).

Let us start with the results for a perturbation such

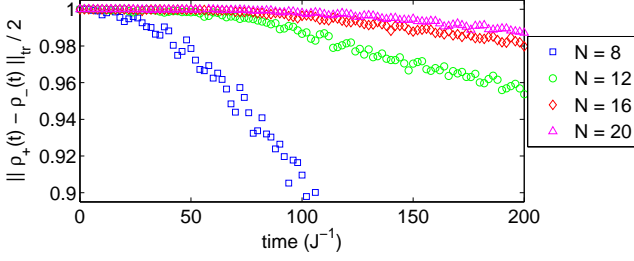


FIG. 2: Robustness of the quantum memory against time-dependent Hamiltonian perturbations: $\mu_0 = 0$ and $\mu_- = J$, $\mu_+ = 1.5J$. The Hamiltonian time-evolution is swapped between $\hat{H}(\mu_-)$ and $\hat{H}(\mu_+)$ every $\delta t = J^{-1}/4$. The figure shows the optimal fidelity as a function of time for different sizes of the chain, N . We take $N_d = 101$ realizations.

that $\hat{H}_0 + \hat{V} = \hat{H}(\mu)$. We take a distribution of μ which consists of N_d discrete points equally spaced in $[\mu_-, \mu_+]$. Figure 1(a,b) displays F_t^{opt} as a function of t for different system sizes. We have chosen μ_{\pm} such that the perturbed Hamiltonians lie inside (a) and outside (b) the topological phase, respectively. In the first case, the decay time of F_t^{opt} does not depend on the size N , whereas in the latter does. This is quantified in panel (c), which displays $t_0(N)$, the time at which a prescribed fidelity threshold [12], F_0 , is crossed versus N . We take a polynomial fit of F_t^{opt} so that $t_0(N)$ is then obtained at the interception of the fitting curve with F_0 . Results are compatible with an exponential growth of the memory time with N . We have also considered inhomogeneous local perturbations obtaining the same qualitative results.

To analyze time-dependent perturbations, we focused on a square wave, $\mu(t) = \bar{\mu} + \delta\mu \cdot \text{sgn}[\sin(2\pi\omega t)]$ where $\{\bar{\mu}, \delta\mu\} = (\mu_+ \pm \mu_-)/2$ is averaged over $N_d = 101$ realizations. In Figure 2 we have taken $\omega = 2J$, which is larger than the Hamiltonian gap (of the order of J). Remarkably, even in this case the memory time grows with the system size N .

These results indicate that the memory can withstand perturbations that keep the system within the topological phase, despite the initial state having plenty of excitations (in terms of each perturbed Hamiltonian). The stability can be traced back (see the appendix) to the fact that for any pair of Hamiltonians H_a and H_b in the topological phase,

$$\langle 0 | \exp(iH_a t) \exp(-iH_b t) | 0 \rangle \approx \langle 1 | \exp(iH_a t) \exp(-iH_b t) | 1 \rangle, \quad (7)$$

where the difference decays exponentially with N ($|0\rangle$ and $|1\rangle$ are the two ground states for the original Hamiltonian, H_0). This means that the excitations generated by any pair of evolutions have almost the same overlap (in modulus and phase) independent on whether they started, in $|0\rangle$ or $|1\rangle$. This appears to be a consequence of the topological nature of our system and therefore should

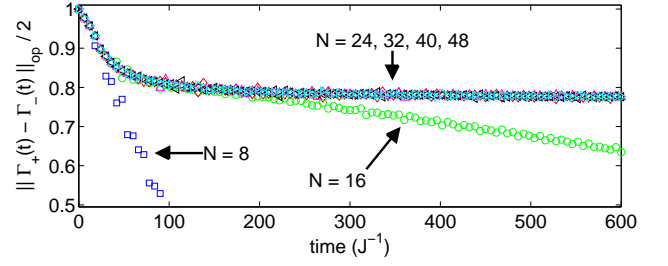


FIG. 3: Optimal Gaussian fidelity as a function of time for different system sizes N : $\mu_0 = 0$ and $\mu_- = J$, $\mu_+ = 1.5J$. We considered at most $N_d = 101$ realizations uniformly distributed in the range $[\mu_-, \mu_+]$; plotted values for $N_d \rightarrow \infty$ are obtained via scaling as $1/N_d$ (see the appendix).

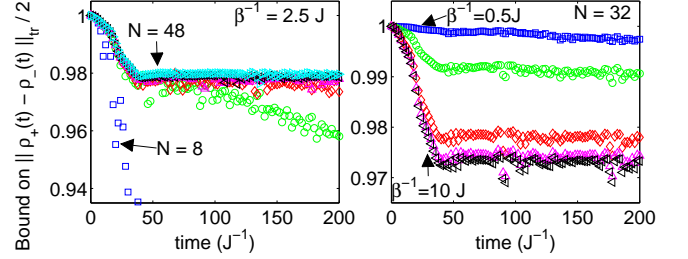


FIG. 4: Upper bound to the optimal fidelity in presence of thermal modes. (left) Temperature is fixed: $\beta^{-1} = 2.5J$ and the figure shows the upper bound as a function of time for different lengths of the chain $N = 8, 16, 24, 32, 40, 48$. (right) Size is fixed: $N = 32$ and the figure shows the upper bound as a function of time for different temperatures $\beta^{-1} = 0.5J, 1.0J, 2.5J, 5J$ and $10J$. We take $N_d = 101$ realizations.

likely be present in other systems as well.

Time-independent perturbations have also been recently considered in [12], obtaining different conclusions. In particular, in their analysis the memory time does not grow exponentially with the system size. The discrepancy originates from their choice of the syndrome based recovery operation [27], which, according to our results, is not the optimal one. Nevertheless, they introduce random site-dependent variations of the chemical potential to localize the excitations and increase the memory time (see also [36, 37]). Our analysis shows that this is not necessary if the optimal recovery operation is used.

We next examine memory performance for a restricted set of Gaussian recovery operations. Figure 3 displays the optimal Gaussian fidelity in the presence of the same perturbations as in Fig. 1(a): the fidelity improves with the size of the system but saturates for sufficiently large N . Remarkably, similar results are obtained when all the modes different from a (i.e. corresponding to non-zero Majorana modes) are initially in thermal equilibrium at a temperature β^{-1} , as shown in Fig. 4. Because we deal with convex combinations of mixed states, we can only plot an upper bound F_t^{up} to the optimal fidelity (see the

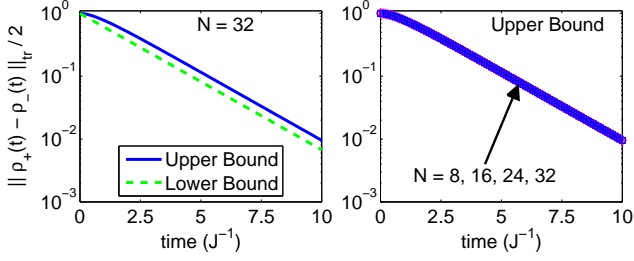


FIG. 5: Effects of particle losses according to equation (8); $\mu_0 = 0$ and $\Gamma = J$. (left) Upper and lower bound to the optimal fidelity as a function of time, showing a clear exponential scaling. (right) Upper bound to the optimal fidelity as a function of time for different system sizes: $N = 8, 16, 24$ and 32 . Results coincide exactly and are indistinguishable.

appendix). For temperatures above the gap, a clear saturation behavior is displayed, see Fig. 4 (left). For temperatures below the gap, our results are not conclusive (not shown), but lowering the temperature while keeping a fixed value of N clearly increases the memory time, as shown in Fig. 4 (right). Thus, the temperature defines an effective size up to which topological protection can occur. These result regarding the Gaussian recovery operation can be understood as follows: (i) although each term in the integral (6) is Gaussian, its sum is not, and thus the density operator is not Gaussian either; (ii) a Gaussian recovery operation can only depend on the covariant matrix, Γ , which for (pure) non-Gaussian states coincides with that of a mixed Gaussian state [38]. Therefore, restricting to Gaussian recoveries has the same effect as considering mixed states, and this explains the similarity between this case and that of finite temperature.

Markovian interaction with a bath. We analyze now the interaction of the system with a bath with which it can interchange particles via a Lindblad master equation:

$$\partial_t \hat{\rho} = -i [\hat{H}_0, \hat{\rho}] + \Gamma \sum_{n=1}^N \left(\hat{d}_n \hat{\rho} \hat{d}_n^\dagger - \frac{1}{2} \{ \hat{d}_n^\dagger \hat{d}_n, \hat{\rho} \} \right). \quad (8)$$

Here $\hat{d}_n = \frac{1}{2}(\hat{c}_{2n-1} + i\hat{c}_{2n})$ annihilates one fermion in the n -th physical site, and \hat{H}_0 is the protecting Hamiltonian. This equation transforms Gaussian states into Gaussian states, and thus can be rewritten in terms of the CM [39].

Given previous works [19], one would expect that the memory time does not scale with the system size. However, since optimal recovery operations have not yet been considered in this context, we investigate whether the result extends to the optimal recovery, and thus compute F_t^{opt} . Unfortunately, the trace-norm appearing in (4) cannot be directly computed in terms of the CM. In order to circumvent this problem, we bound F_t^{opt} with $\frac{1}{2} \|\hat{\rho}_{x,+}(t) - \hat{\rho}_{x,-}(t)\|_{\text{tr}} \leq (1 - F_U(\hat{\rho}_{x,+}, \hat{\rho}_{x,-})^2)^{1/2}$ [6], where F_U is the Uhlmann fidelity [6], which for Gaussian states is a function of their CM (see the appendix).

Results in figure 5 demonstrate that the information is corrupted at a rate which does not depend on the system size. As expected, the exchange of single particles with a bath mixes states of different parity, and thus gives rise to irreversible losses.

Conclusions. We have studied the possibility of storing quantum states in a Kitaev chain in the presence of perturbations and decoherence. In particular, we have investigated for how long the information is still present somewhere in the Hilbert space corresponding to the chain. We have derived a formula that quantifies the optimal (memory) fidelity for both general and Gaussian recovery operations. For both, static and time-dependent Hamiltonian perturbations within the topological phase, we have gathered numerical evidence that the memory time grows exponentially with the system size. We have identified the condition (7) which is responsible for this result. For Gaussian recovery operations or at finite temperature, the memory time saturates with the system size. We have also confirmed that when particle losses are present, the memory time is independent from the system size. We believe that our results can be extended to other topological superconductors based on Majorana zero energy modes, like the $p_x + ip_y$ model [15, 16], as well as that our methods could have applications in the study of fractional quantum Hall systems. In particular, it will be very interesting to investigate more in detail the general relation between the memory protection against dynamical perturbations, as analyzed here and illustrated by condition 7), with the topological character of the Hamiltonian responsible for the dynamics.

Acknowledgements. We gratefully acknowledge fruitful discussions with G. Giedke, V. Giovannetti, B. Horstmann, C. Kraus, F. Pastawski. Special thanks for unvaluable support to H.-H. Tu. Part of this work has been supported by the European Community's Seventh Framework Programme (FP7/2007-2013) under grant agreement no. 247687 (IP-AQUTE). LM is supported by Regione Toscana POR FSE 2007-2013.

Appendix: Fermionic Gaussian States

The formalism of fermionic gaussian states (FGS) [28] is particularly useful in the treatment of quadratic fermionic theories, which include a wide class of topological materials [15]. Not only FGS comprise the ground states and thermal states of such Hamiltonians (via Bogoliubov transform) but also they describe dynamical evolution under some master equations (exactly) [39] or in presence of moderate interactions (approximately) [40]. For a N modes system, calculations are restricted on a space scaling only as N rather than exponentially. Indeed, these states are fully characterized by the sole (antisymmetric and real valued) covariance matrix (CM), i.e. the expectation values of quadratic com-

binations of fields, whereas all higher moments can be deduced via Wick theorem [41].

Given N fermionic modes, we can conveniently rewrite the $2N$ canonical Dirac fermionic operators $\{\hat{d}_i^{(\dagger)}\}_{i=1\dots N}$ (with $\{\hat{d}_i, \hat{d}_j\} = 0$; $\{\hat{d}_i, \hat{d}_j^\dagger\} = \delta_{i,j}$) in terms of Majorana operators, i.e. fermionic operators which are real, Hermitian and unitary:

$$\hat{c}_{j,1} = \hat{d}_j + \hat{d}_j^\dagger; \quad \hat{c}_{j,2} = -i(\hat{d}_j - \hat{d}_j^\dagger); \quad \{\hat{c}_m, \hat{c}_n\} = 2\delta_{m,n}, \quad (9)$$

where $m \in \{(1,1), \dots, (N,2)\}$ glues two sub-indices together for brevity. By a bit of simple algebra, Eq.(1) of the Letter is seen to be a rewriting of

$$\hat{H}(\mu) = \sum_{j=1}^{N-1} \left(-J \hat{d}_j^\dagger \hat{d}_{j+1} + \Delta \hat{d}_j^\dagger \hat{d}_{j+1}^\dagger + \text{h.c.} \right) - \mu \sum_{j=1}^N \hat{d}_j^\dagger \hat{d}_j,$$

where $J = \Delta = 1$. Canonical transformations can be represented by orthogonal real matrices, $\hat{c}_k \rightarrow \hat{c}'_k = \sum_l O_{k,l} \hat{c}_l$, as well as by a unitary rotation $\hat{c}'_k = \hat{U} \hat{c}_k \hat{U}^\dagger$ in Fock space [28]: in the case of $O \in O(2m)$, i.e. $\det O = 1$, the relation reads $O = \exp(A) \Leftrightarrow \hat{U} = \exp(-A_{\alpha,\beta} \hat{c}_\alpha \hat{c}_\beta / 4)$ apart from an arbitrary phase. The number parity operator reads $\hat{P} = (-1)^{\sum_j \hat{d}_j^\dagger \hat{d}_j} = i^N \prod_k \hat{c}_k$ and is almost invariant under canonical transformations: $\hat{P}' = \det O \cdot \hat{P}$.

A N -modes FGS is a N -fermions state which has a density operator of the form $\hat{\rho} = \prod_{\alpha=1}^N \hat{\rho}_\alpha$, with

$$\hat{\rho}_\alpha = \frac{e^{-\beta_\alpha \hat{d}_\alpha^\dagger \hat{d}_\alpha}}{1 + e^{-\beta_\alpha}} = \frac{e^{-\frac{i}{4} \beta_\alpha (\hat{c}_{\alpha,1} \hat{c}_{\alpha,2} - \hat{c}_{\alpha,2} \hat{c}_{\alpha,1})}}{2 \cosh(\beta_\alpha / 2)} = \frac{\hat{1} - i \lambda_\alpha \hat{c}_{\alpha,1} \hat{c}_{\alpha,2}}{2}, \quad (10)$$

where $\lambda_\alpha = \tanh(\beta_\alpha / 2)$, and the $\hat{a}_\alpha^{(\dagger)}$ ($\hat{c}_{\alpha,\sigma}$) are the eigenmodes of the density operator. One can easily verify that $\text{Tr} \hat{\rho} = 1$, whereas $\text{Tr} \hat{\rho}^2 = \prod_\alpha (1 + \lambda_\alpha^2) / 2$, i.e. the state is pure if and only if $\lambda_\alpha = \pm 1$; moreover, $\hat{\rho}$ is positive – and thus a well-defined density operator – if and only if $\lambda_\alpha \in [-1, 1]$. FGS automatically satisfy the superselection rule of the fermionic parity \hat{P} , and therefore their density matrices can be expressed as a direct sum $\hat{\rho} = \hat{\rho}_{\text{even}} \oplus \hat{\rho}_{\text{odd}}$.

The skew-symmetric covariance matrix (CM) of a FGS $\hat{\rho}$ is defined as the table of quadratic expectation values:

$$\Gamma_{m,n} = \frac{i}{2} \text{Tr} [\hat{\rho} (\hat{c}_m \hat{c}_n - \hat{c}_n \hat{c}_m)]; \quad \Gamma = \bigoplus_\alpha \begin{pmatrix} 0 & -\lambda_\alpha \\ \lambda_\alpha & 0 \end{pmatrix}, \quad (11)$$

where the second expression is given in the eigenbasis of Eq.(10). Under a canonical transformation O , the CM transforms as $\Gamma' = O \Gamma O^T$. The CM completely characterizes the properties of a FGS, as elegantly stated by the following reformulation of the Wick's theorem [41]:

$$i^p \text{Tr} [\hat{\rho} \hat{c}_{\alpha_1} \dots \hat{c}_{\alpha_{2p}}] = \text{Pf} \left[\Gamma|_{\alpha_1 \dots \alpha_{2p}} \right], \quad (12)$$

where $\Gamma|_{\alpha_1 \dots \alpha_{2p}}$ is the restriction of Γ to the modes $\{\alpha_1 \dots \alpha_{2p}\}$, and Pf denotes its Pfaffian. This allows to simulate FGS efficiently with classical computers.

The squared overlap of two FGS $\hat{\rho}$ and $\hat{\sigma}$ is [28]:

$$\text{Tr} [\hat{\rho} \hat{\sigma}] = + \sqrt{\det \left[\frac{1 - \Gamma_\rho \Gamma_\sigma}{2} \right]}, \quad (13)$$

Moreover, generalizations of formula 13 can be derived for any two Gaussian operators, as explained in [28]. Because the time-evolution $\hat{U}(t)$ under a quadratic Hamiltonian \hat{H} is a Gaussian operator, such formulas for $\text{Tr} [\hat{\rho} \hat{U}(t)]$ and $\text{Tr} [\hat{U}'(t) \hat{U}''(t)]$ have been widely used in the Letter. Moreover, the CM of $\hat{U}(t) \hat{\rho}(0) \hat{U}(t)^\dagger$ is: $\Gamma(t) = O(t) \Gamma(0) O(t)^T$, where $O(t) = e^{-Tt}$ and T is the real skew-symmetric matrix such that $\hat{H} = \frac{i}{4} \sum_{j,k} T_{j,k} \hat{c}_j \hat{c}_k$.

Also the Uhlmann fidelity among mixed Gaussian states, $F_U(\hat{\rho}, \hat{\sigma}) = \text{Tr} \sqrt{\hat{\rho}^{1/2} \hat{\sigma} \hat{\rho}^{1/2}}$, can be efficiently computed via their CM's. By using Eq.(10), we can define \hat{H}_ρ such that $\hat{\rho}^{1/2} = \exp(-\hat{H}_\rho) / \sqrt{\text{Tr} \exp(-2\hat{H}_\rho)}$ and the corresponding imaginary-time evolution of the state $\hat{\sigma}$ [40]:

$$\hat{\rho}^{1/2} \hat{\sigma} \hat{\rho}^{1/2} = \text{Tr} [\hat{\rho} \hat{\sigma}] \cdot \hat{\sigma}_I(\tau = 1); \quad \hat{\sigma}_I(\tau) = \frac{e^{-\hat{H}_\rho \tau} \hat{\sigma} e^{-\hat{H}_\rho \tau}}{\text{Tr} [e^{-2\hat{H}_\rho \tau} \hat{\sigma}]}. \quad (14)$$

Since $\hat{\sigma}_I(\tau)$ is still a Gaussian state, whose CM can be efficiently computed [40], the trace of its square root in F_U can be calculated by looking again at Eq. (10) as above.

Appendix: Optimal Recovery Operation

We present the derivation of formula (4) of the Letter, which describes the fidelity of the optimal recovery operation acting after a given decoherence map, rewritten here for reading convenience:

$$F_t^{\text{opt}} = \max_{\mathcal{R}_t} F(\mathcal{R}_t) = \frac{2}{3} + \frac{1}{6} \|\hat{\rho}_{x,+}(t) - \hat{\rho}_{x,-}(t)\|_{\text{tr}}; \quad (15)$$

where $\hat{\rho}_{x,\pm}(t) = \mathcal{D}_t(\hat{\Psi}_{x,\pm})$ and $\hat{\Psi}_{x,\pm} = (\hat{1} \pm \hat{\sigma}'_x) / 2$.

We first show that the fidelity of any recovery operation is upper bounded: $F(\mathcal{R}_t) \leq F_t^{\text{opt}} \forall \mathcal{R}_t$ and then construct an explicit recovery operation, $\mathcal{R}_t^{\text{opt}}$, which achieves the upper bound.

Before presenting the proof we recall that for any bounded Hermitian operator \hat{X} the trace norm is $\|\hat{X}\|_{\text{tr}} = \max_{\hat{H}} \text{tr}(\hat{H} \hat{X})$, and the maximization is restricted to Hermitian operators fulfilling $\|\hat{H}\|_{\text{op}} \leq 1$, where $\|\hat{X}\|_{\text{op}}$ denotes the maximum singular value of \hat{X} .

Moreover, $F(\mathcal{R}_t)$ is an average over the Bloch surface (see Eq. (3) in the Letter) which is best expressed as [33]:

$$F(\mathcal{R}_t) = \frac{1}{2} + \frac{1}{12} \sum_{\alpha=x,y,z} \text{tr}[\hat{\sigma}'_\alpha \mathcal{T}_t(\hat{\sigma}'_\alpha)]. \quad (16)$$

We derive the upper bound. Because of the contractivity of the trace distance under \mathcal{R}_t [6], the inequality

$$\text{tr}[\hat{\sigma}'_\alpha \mathcal{T}_t(\hat{\sigma}'_\alpha)] \leq \|\hat{\sigma}'_\alpha\|_{\text{op}} \|\mathcal{T}_t(\hat{\sigma}'_\alpha)\|_{\text{tr}} \leq 1 \cdot \|\mathcal{D}_t(\hat{\sigma}'_\alpha)\|_{\text{tr}}$$

holds, from which we obtain:

$$F(\mathcal{R}_t) \leq \frac{1}{2} + \frac{1}{12} \sum_{\alpha=x,y,z} \|\hat{\rho}_{\alpha,+}(t) - \hat{\rho}_{\alpha,-}(t)\|_{\text{tr}}. \quad (17)$$

Let us now specify (17) to the case of \mathcal{D}_t not acting on the fermionic mode A_0 . The operator $\hat{H}_z \doteq \hat{a}\hat{a}^\dagger - \hat{a}^\dagger\hat{a}$ is Hermitian and $\|\hat{H}_z\|_{\text{op}} \leq 1$; moreover $\text{tr}[\hat{H}_z \hat{\rho}_{z,\pm}(t)] = \pm 1$. Thus we have:

$$\begin{aligned} 2 &= \text{tr}[\hat{H}_z(\hat{\rho}_{z,+}(t) - \hat{\rho}_{z,-}(t))] \leq \\ &\leq \|\hat{\rho}_{z,+}(t) - \hat{\rho}_{z,-}(t)\|_{\text{tr}} \leq \|\hat{\Psi}_{z,+} - \hat{\Psi}_{z,-}\|_{\text{tr}} = 2 \end{aligned}$$

so that $\|\hat{\rho}_{z,+}(t) - \hat{\rho}_{z,-}(t)\|_{\text{tr}} = 2$. Furthermore, since \mathcal{D}_t does not act on the ancilla, we can write $\hat{\rho}_{y,\tau}(t) = \hat{V}_{xy}\hat{\rho}_{x,\tau}(t)\hat{V}_{xy}^\dagger$, where $\hat{V}_{xy} \doteq e^{-i\pi\hat{a}^\dagger\hat{a}/2}$. Therefore:

$$\|\hat{\rho}_{x,+}(t) - \hat{\rho}_{x,-}(t)\|_{\text{tr}} = \|\hat{\rho}_{y,+}(t) - \hat{\rho}_{y,-}(t)\|_{\text{tr}} \quad (18)$$

The bound $F(\mathcal{R}_t) \leq F_t^{\text{opt}} \forall \mathcal{R}_t$ follows from the combination of (17) with these considerations.

The recovery map $\mathcal{R}_t^{\text{opt}}$ which achieves $F(\mathcal{R}_t) = F_t^{\text{opt}}$ is in the form:

$$\mathcal{R}_t^{\text{opt}}(\hat{\rho}(t)) = \frac{1}{2}\hat{1} \text{tr}[\hat{\rho}(t)] + \frac{1}{2} \sum_{\alpha} \hat{\sigma}'_{\alpha} \text{tr}[\hat{H}_{\alpha}\hat{\rho}(t)]. \quad (19)$$

and the operators \hat{H}_{α} are such that $\text{tr}[\hat{H}_{\alpha}\mathcal{D}_t(\hat{\sigma}'_{\alpha})] = \|\mathcal{D}_t(\hat{\sigma}'_{\alpha})\|_{\text{tr}}$. \hat{H}_z has already been defined. The \hat{H}_{α} can be interpreted as the observables to be measured in $\hat{\rho}(t)$ in order to reconstruct $\hat{\rho}_q$

Let us rewrite

$$\hat{\rho}_{x,+}(t) - \hat{\rho}_{x,-}(t) = \hat{a}\hat{R} + \hat{R}^\dagger\hat{a}^\dagger; \quad \hat{R} = \mathcal{D}_t(-\hat{b})$$

We write the most general Hermitian operator:

$$\hat{H}_x = \hat{a}\hat{S}_1 + \hat{S}_1^\dagger\hat{a}^\dagger + \hat{a}^\dagger\hat{a}\hat{S}_2 + \hat{a}\hat{a}^\dagger\hat{S}_3$$

which must satisfy $\hat{H}_x^\dagger\hat{H}_x \leq \mathbb{1}$. We get

$$\text{tr}[\hat{H}_x(\hat{a}\hat{R} + \hat{R}^\dagger\hat{a}^\dagger)] = \text{tr}[(\hat{S}_1\hat{R}^\dagger + \hat{R}\hat{S}_1^\dagger)\hat{a}^\dagger\hat{a}]$$

Using the left polar decomposition $\hat{R} = \hat{P}\hat{U}$, where $\hat{P} = \sqrt{\hat{R}\hat{R}^\dagger}$ is positive semi-definite and \hat{U} is unitary, we have that the maximum is attained when $\hat{S}_1 = \hat{U}$, and $\hat{S}_2 = \hat{S}_3 = 0$. Therefore, the maximum is achieved by:

$$\hat{H}_x = \hat{a}\hat{U} + \hat{U}^\dagger\hat{a}^\dagger; \quad \hat{H}_y = -i\hat{a}\hat{U} + i\hat{U}^\dagger\hat{a}^\dagger.$$

Furthermore, since both \hat{a} and \hat{R} change the fermionic parity, $\hat{H}_{x,y}$ do not. They also fulfill:

$$\text{tr}[\hat{H}_{\alpha}\hat{\rho}_{\alpha,\pm}(t)] = \pm \frac{1}{2} \|\hat{\rho}_{x,+}(t) - \hat{\rho}_{x,-}(t)\|_{\text{tr}}; \quad \alpha = x, y$$

from which $\text{tr}[\hat{H}_{\alpha}\mathcal{D}_t(\hat{\sigma}'_{\alpha})] = \|\mathcal{D}_t(\hat{\sigma}'_{\alpha})\|_{\text{tr}}$ follows.

The optimal recovery map (19) is linear, trace preserving, and it also preserves the fermionic parity, since \hat{H}_{α} do. For it to be a valid quantum channel we have only to show that it is completely positive. We construct a unitary operator acting on all the fermionic modes, \hat{W} , such that $\mathcal{R}_t^{\text{opt}}(\hat{\rho}) = \text{tr}[\hat{W}\hat{\rho}\hat{W}^\dagger]$, where the trace is taken over the fermionic degrees of freedom which are not part of the qubit. The operator is:

$$\hat{W} = \frac{1}{8} \left[\hat{1} + \sum_{\alpha=x,y,z} \hat{\sigma}'_{\alpha} \hat{H}_{\alpha} \right]. \quad (20)$$

Using that $\hat{H}_{\alpha}^2 = \hat{1}$ and $\hat{H}_{\alpha}\hat{H}_{\beta} = i\epsilon_{\alpha,\beta,\gamma}\hat{H}_{\gamma}$, where $\epsilon_{\alpha,\beta,\gamma}$ is the Levi-Civita symbol, one can show that \hat{W} is unitary and that it satisfies $\mathcal{R}_t^{\text{opt}}(\hat{\rho}) = \text{tr}[\hat{W}\hat{\rho}\hat{W}^\dagger]$. Furthermore, $F(\mathcal{R}_t^{\text{opt}})$ saturates the bound in (4).

Appendix: Gaussian Recovery Operation

We present the derivation of formula (5) of the Letter, which describes the fidelity of the optimal Gaussian recovery operation acting after a given decoherence map, rewritten here for reading convenience:

$$F_{G,t}^{\text{opt}} = \max_{\mathcal{R}_t \text{ is Gaussian}} = \frac{2}{3} + \frac{1}{6} \|\Gamma_{x,+}(t) - \Gamma_{x,-}(t)\|_{\text{op}}.$$

The proof is similar to that in the previous section. In this case, we need to explicitly consider the fact that the qubit is composed of fermions. In particular, we have to consider what happens if the decoherence channel changes the parity of the state. This occurs, for instance, when decoherence is caused by the interchange of particles with a reservoir, as described by $\mathcal{D}_t(\hat{\rho}) = (\hat{b} + \hat{b}^\dagger)\hat{\rho}(\hat{b} + \hat{b}^\dagger)$. The final state contains all the information about the initial state of the qubit, even if now it has odd parity. The problem, that could be overlooked in the previous section, arises in this section because the Gaussian recovery operation cannot act independently on the different parity sectors of the state, whereas a general recovery operation can.

We denote \hat{m}_1, \hat{m}_2 the zero-energy modes of one Kitaev chain and \hat{m}_3 and \hat{m}_4 the modes of a decoherence-free ancilla. We express the Pauli operators of the qubit as:

$$\hat{\sigma}_x'' = (\hat{a}^\dagger - \hat{a})(\hat{b}^\dagger + \hat{b}) = i\hat{c}_3\hat{c}_2; \quad (21)$$

$$\hat{\sigma}_y'' = -i(\hat{a}^\dagger + \hat{a})(\hat{b}^\dagger + \hat{b}) = i\hat{c}_3\hat{c}_1; \quad (22)$$

$$\hat{\sigma}_z'' = \hat{a}^\dagger\hat{a} - \hat{a}\hat{a}^\dagger = i\hat{c}_1\hat{c}_2. \quad (23)$$

where the modes $\hat{a}^{(\dagger)}$ and $\hat{b}^{(\dagger)}$ have been defined in the Letter. Note the difference with the $\hat{\sigma}'_{\alpha}$ in Eq. (2) of the Letter. Since the $\hat{\sigma}_{\alpha}''$ act on both the parity sectors of the qubit, they allow the recovery operation independently of whether the parity has been changed or not.

We recall that the action of a general Gaussian channel transforms a Gaussian M -modes state with CM Γ into a N -modes state with CM $\Gamma' = B\Gamma B^T + A$ (see [28]). B and A are $2N \times 2M$ and $2N \times 2N$ matrices chosen such that Q , defined as:

$$Q = \begin{pmatrix} A & B \\ -B^T & 0 \end{pmatrix} \quad (24)$$

satisfies $Q^T Q \leq \mathbb{1}$; A must be skew-symmetric.

We denote $\mathcal{R}_{G,t}$ the Gaussian recovery operation, and $\mathcal{T}_{G,t} = \mathcal{R}_{G,t} \circ \mathcal{D}_t$. Moreover, we define:

$$\Delta_\alpha = \Gamma_{\mathcal{D}_t(\hat{\Psi}_{\alpha,+})} - \Gamma_{\mathcal{D}_t(\hat{\Psi}_{\alpha,-})}, \quad (25)$$

$$\Delta_\alpha^{\text{out}} = \Gamma_{\mathcal{T}_{G,t}(\hat{\Psi}_{\alpha,+})} - \Gamma_{\mathcal{T}_{G,t}(\hat{\Psi}_{\alpha,-})} = B\mathcal{R}\Delta_\alpha B_{\mathcal{R}}^T, \quad (26)$$

the difference of covariance matrices corresponding to the states after the decoherence channel and after the recovery operation, respectively. Note that the matrices Δ_α are $2N \times 2N$ matrices, whereas the matrices $\Delta_\alpha^{\text{out}}$ are 4×4 matrices. The assumption that the decoherence channel does not act on the first two Majorana modes $\hat{c}_{1,2}$ is reflected by some properties of Δ_α which are best expressed considering the block structure:

$$\Delta_\alpha = \begin{pmatrix} K'_\alpha & -L_\alpha^T \\ L_\alpha & K''_\alpha \end{pmatrix}, \quad (27)$$

where K', L and K'' are 2×2 , $2(N-1) \times 2$, and $2(N-1) \times 2(N-1)$ matrices, respectively. We obtain:

$$K'_z = -2J; \quad L_x = \begin{pmatrix} \vec{l}_1 & \vec{l}_2 \end{pmatrix}; \quad L_y = L_x J; \quad J = \begin{pmatrix} 0 & -1 \\ 1 & 0 \end{pmatrix}; \quad (28)$$

where $\vec{l}_{1,2}$ are column vectors. Additionally, L_z , $K'_{x,y}$ and $K''_{x,y}$ are zero matrices. Thus:

$$\|\Delta_x\|_{\text{opt}} = \|\Delta_y\|_{\text{opt}} = \|L_x\|_{\text{opt}} \leq 2. \quad (29)$$

We can now show that $F(\mathcal{R}_{G,t}) \leq F_{G,t}^{\text{opt}} \forall \mathcal{R}_{G,t}$. The starting point is equation (16), modified as follows:

$$F_{G,t} = \frac{1}{2} + \frac{1}{12} \sum_{\alpha=x,y,z} \text{tr}[\hat{\sigma}''_\alpha \mathcal{T}_{G,t}(\hat{\sigma}'_\alpha)]. \quad (30)$$

Noting that the $\hat{\sigma}''_\alpha$ are quadratic in the Majorana operators and recalling the definition of CM, we obtain:

$$\text{tr}[\hat{\sigma}''_\alpha \mathcal{T}_{G,t}(\hat{\sigma}'_\alpha)] = (\Delta_\alpha^{\text{out}})_{\beta_1, \beta_2} \leq \|\Delta_\alpha^{\text{out}}\|_{\text{opt}}, \quad (31)$$

where $(\beta_1, \beta_2) = (3, 2), (3, 1)$, and $(1, 2)$ for $\alpha = x, y, z$, respectively. The most general Gaussian recovery operator $\mathcal{R}_{G,t}$ yields:

$$\|\Delta_\alpha^{\text{out}}\|_{\text{op}} = \|B_{\mathcal{R}} \Delta_\alpha B_{\mathcal{R}}^T\|_{\text{op}} \leq \|\Delta_\alpha\|_{\text{op}} \quad (32)$$

given that $Q^T Q \leq \mathbb{1}$. Since $2 \geq \|\Delta_z\|_{\text{op}} \geq (\Delta_z)_{1,2} = (K_z)_{1,2} = 2$, we get that $\|\Delta_z\|_{\text{op}} = 2$. Using (29) we obtain the desired bound.

We now provide an explicit Gaussian recovery operation which attains the bound. The recovery operation consists of the application of a Gaussian unitary operation \hat{W}_G to the system and in subsequently tracing out $N-2$ modes of the system. To define \hat{W}_G , consider the singular value decomposition of $L_x = U\Sigma V^T$, where U (V) is a unitary $2(N-1) \times 2(N-1)$ (2×2) matrix and Σ is a $2(N-1) \times 2$ matrix. Clearly, it is also possible to construct U' and V' such that $L_x = U'\Sigma'V'$ and Σ' has at most two elements different from zero, $\Sigma'_{1,2} \geq \Sigma'_{2,1} \geq 0$, named the singular values of L_x . We define \hat{W}_G to be the unitary transformation which is represented by an orthogonal transformation $V' \oplus U'$:

$$\hat{W}_G \vec{c} \hat{W}_G^\dagger = (V' \oplus U') \vec{c} \quad (33)$$

Physically, \hat{W}_G rotates all the information between ancilla and system into the first two modes of the system. The other modes can be now traced out. Summarizing:

$$\mathcal{R}_{G,t}^{\text{opt}}(\hat{\rho}) = \text{tr}[\hat{W}_G \hat{\rho} \hat{W}_G^\dagger] \quad (34)$$

The CM of $\mathcal{R}_{G,t}^{\text{opt}}(\hat{\rho})$ is a function of Γ , the CM of $\hat{\rho}$:

$$\Gamma_{\mathcal{R}_{G,t}^{\text{opt}}(\hat{\rho})} = [(V' \oplus U') \Gamma (V'^T \oplus U'^T)]|_{(1-4), (1-4)}. \quad (35)$$

Finally, let us prove that $F(\mathcal{R}_{G,t}^{\text{opt}})$ saturates the bound. Denote $\mathcal{T}_{G,t}^{\text{opt}} = \mathcal{R}_{G,t}^{\text{opt}} \circ \mathcal{D}_t$. Clearly,

$$\sum_{\alpha=x,y,z} \text{tr}[\hat{\sigma}''_\alpha \mathcal{T}_{G,t}^{\text{opt}}(\hat{\sigma}'_\alpha)] = (\Delta_x^{\text{out}})_{3,2} + (\Delta_y^{\text{out}})_{3,1} + (\Delta_z^{\text{out}})_{1,2}.$$

By construction of \hat{W}_G , $(\Delta_x^{\text{out}})_{3,2} = \|\Delta_x\|_{\text{op}}$. Since J commutes with every 2×2 orthogonal matrix, $(\Delta_y^{\text{out}})_{3,1} = \|\Delta_y\|_{\text{op}} = \|\Delta_x\|_{\text{op}}$. Finally, $(\Delta_z^{\text{out}})_{1,2} = (\Delta_z)_{1,2} = 2$ because the orthogonal transformation V' leaves the covariance matrix of the fermionic mode A_0 unchanged. Together with equation (30), this shows that the recovery operation $\mathcal{R}_{G,T}^{\text{opt}}$ saturates the bound in (5).

Appendix: Some Details on Hamiltonian Perturbations

We study the effect of the disturbance described in Eq. (6) of the Letter; we use formula (4). For simplicity, let us discretize the integral $(\Delta\nu)^{-1} \int d\nu \rightarrow N_d^{-1} \sum_1^{N_d}$ and define the $N_d \times N_d$ matrices G_0 and G_1 :

$$[G_\tau]_{j,k} = \langle g_\tau | e^{i\hat{H}_j \tau} e^{-i\hat{H}_k \tau} | g_\tau \rangle; \quad \hat{H}_j \doteq \hat{H}_0 + \hat{V}_j; \quad (36)$$

with notation taken from the Letter. We now show that:

$$\frac{1}{2} \|\hat{\rho}_{x,+}(t) - \hat{\rho}_{x,-}(t)\|_{\text{tr}} = \left\langle \sqrt{G_0/N_d}, \sqrt{G_1/N_d} \right\rangle \quad (37)$$

where $\langle \cdot, \cdot \rangle$ is the Hilbert-Schmidt inner product for matrices: $\langle A, B \rangle = \text{tr}[B^\dagger A]$. It follows that perfect recoverability, namely $\|\hat{\rho}_{x,+}(t) - \hat{\rho}_{x,-}(t)\|_{\text{tr}} = 2$, is equivalent to

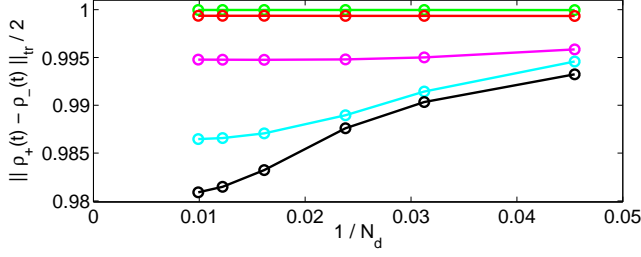


FIG. 6: Dependence of F_t^{opt} on N_d . These data refer to the topological perturbation of figure 1 of the Letter: $N = 32$, $\mu_0 = 0$, $\mu_- = J$, $\mu_+ = 1.5J$. The scaling is shown for five times. From up to down: $24J^{-1}$, $54J^{-1}$, $174J^{-1}$, $354J^{-1}$, $474J^{-1}$. Data show a convergence behaviour for $N_d \rightarrow \infty$.

$G_0 = G_1$, i.e. to the two topological sectors of the theory “behaving” in the same way.

First, a simple inspection shows that $G_\sigma = G_\sigma^\dagger$, $G_\sigma > 0$ and $\|\sqrt{G_\sigma/N_d}\|_{\text{HS}} = 1$. Let us consider the states $|\pm\rangle = (|g_0\rangle \pm |g_1\rangle)/\sqrt{2}$ and use them to define the overlap matrix M :

$$M = \begin{pmatrix} M^{(+,+)} & M^{(+,-)} \\ M^{(-,+)} & M^{(-,-)} \end{pmatrix} = \frac{1}{2} \begin{pmatrix} G_0 + G_1 & G_0 - G_1 \\ G_0 - G_1 & G_0 + G_1 \end{pmatrix}. \quad (38)$$

with $M_{j,k}^{(\tau,\tau')} = \langle \tau | e^{i\hat{H}_j t} e^{-i\hat{H}_k t} | \tau' \rangle$. The second equality follows from the assumption of a decoherence-free mode. Let us now consider the set of $2N_d$ states: $\mathcal{C} = \{e^{-i\hat{H}_j t} |+\rangle\}_{j=1}^{N_d} \cup \{e^{-i\hat{H}_j t} |-\rangle\}_{j=1}^{N_d}$ and an orthonormal basis $\mathcal{B} = \{|x_j\rangle\}_{j=1}^{N_B}$ such that: $\text{span } \mathcal{B} \equiv \text{span } \mathcal{C}$. A matrix Y representing the basis change: $e^{-i\hat{H}_k t} |+\rangle = \sum_q Y_{k,q}^* |x_q\rangle$ and $e^{-i\hat{H}_k t} |-\rangle = \sum_q Y_{N_d+k,q}^* |x_q\rangle$ is defined by $Y Y^\dagger = M$ and can be computed via the eigenvalue decomposition of M . Given V unitary and D diagonal matrix such that: $M = V D V^\dagger$, a Y defined as $Y \doteq V \sqrt{D}$ is one such possible basis change. A simple algebra leads to:

$$\frac{1}{2} \|\hat{\rho}_{x,+}(t) - \hat{\rho}_{x,-}(t)\|_{\text{tr}} = \frac{1}{2N_d} \left\| Y^\dagger \begin{pmatrix} \mathbb{I} & 0 \\ 0 & -\mathbb{I} \end{pmatrix} Y \right\|_{\text{tr}} \quad (39)$$

We can obtain a more explicit expression of Y considering the eigenvalue decomposition of G_σ : $G_\sigma = V_\sigma D_\sigma V_\sigma^\dagger$ and observing that the matrix:

$$V = \begin{pmatrix} V_0 & V_1 \\ V_0 & -V_1 \end{pmatrix} \quad (40)$$

diagonalizes M . Some simple algebra shows that the singular values of $Y^\dagger \begin{pmatrix} \mathbb{I} & 0 \\ 0 & -\mathbb{I} \end{pmatrix} Y$ are two-fold degenerate and coincide with the singular values of $\sqrt{G_0 G_1}$. Equation (37) follows from the positivity of G_σ .

The numerical computation of G_σ is efficient when \hat{H}_j is a quadratic Hamiltonian so that $\hat{U}_{j,k} \doteq e^{i\hat{H}_j t} e^{-i\hat{H}_k t}$

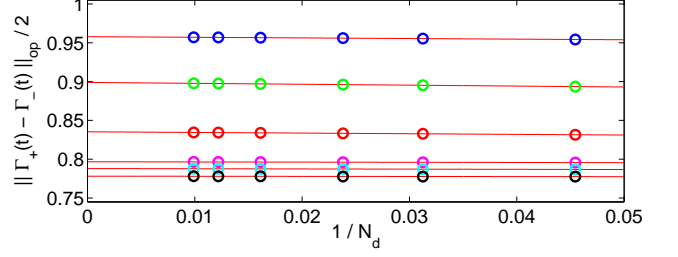


FIG. 7: Dependence of $F_{G,t}^{\text{opt}}$ on $1/N_d$. These data refer to the topological perturbation of figure 1 of the Letter: $N = 32$, $\mu_0 = 0$, $\mu_- = J$, $\mu_+ = 1.5J$. The scaling is shown for five times. From up to down: $12J^{-1}$, $24J^{-1}$, $54J^{-1}$, $174J^{-1}$, $354J^{-1}$, $474J^{-1}$. Data show a N_d^{-1} dependence: the $N_d \rightarrow \infty$ value is extrapolated with a linear fit (thin red lines).

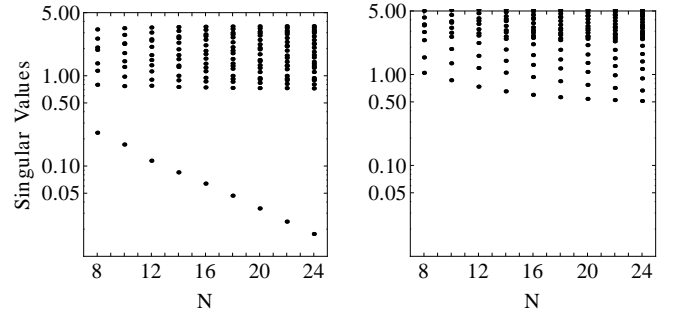


FIG. 8: Singular values of the matrix in equation (41). (Left) The quench Hamiltonians are in the topological phase: $\mu_0 = 0$, $\mu_j = J$, $\mu_k = 1.5J$. (Right) The quench Hamiltonians are not in the topological phase: $\mu_0 = 0$, $\mu_j = 2.5J$ and $\mu_k = 3.0J$.

is a Gaussian operator ($\hat{\rho}_\sigma = |g_\sigma\rangle\langle g_\sigma|$ is FGS) and thus $[G_\sigma]_{j,k}$ is a function of the CM of $\hat{\rho}_\sigma$ and $\hat{U}_{j,k}$. We warn the reader interested in reproducing the data that some care is required in order to obtain the proper phase.

We checked the possibility of using the data to obtain information regarding the limit $N_d \rightarrow \infty$. In figure 6 we show the dependence of F_t^{opt} for different values of N_d ; data show a clear convergence behaviour, even if the functional form of such scaling was not found. In figure 7 we show the dependence of $F_{G,t}^{\text{opt}}$ on N_d ; data show a clear N_d scaling, which allowed us to take the limit $N_d \rightarrow \infty$ with a linear fit.

In the Letter we provide numerical evidence that the memory time of the system increases exponentially while letting the system size $N \rightarrow \infty$, which is equivalent to $X \doteq G_0 - G_1 \xrightarrow{N \rightarrow \infty} 0$. We first observe that:

$$|X_{j,k}| \propto \left| \text{pf} \left[\frac{\Gamma_0 + \Gamma_1}{2} + \frac{\Upsilon}{\text{tr}[\hat{U}_{j,k}(t)]} \right] \right|; \quad (41)$$

where Γ_σ is the CM of $\hat{\rho}_\sigma$ and Υ is the CM of $\hat{U}_{j,k}$; we assume $\text{tr}[\hat{U}_{j,k}(t)] \neq 0$ in order to avoid lengthy regu-

larized expressions. The proportionality factor between l.h.s. and r.h.s. is bounded by 1. Direct numerical inspection of the matrices shows that $X_{j,k} \xrightarrow{N \rightarrow \infty} e^{-N}$ because $\frac{1}{2}(\Gamma_0 + \Gamma_1) + \Upsilon/\text{tr}[\hat{U}_{j,k}(t)]$ has two singular values which scale exponentially to zero (see figure 8). This is clear when $\hat{U}_{j,k} = \mathbb{I}$ and $\Upsilon = 0$ since $\Gamma_0 + \Gamma_1$ has two zero eigenvalues corresponding to the zero-energy modes of the Hamiltonian H_0 . When $\hat{U}_{j,k} \neq \mathbb{I}$ it would be tempting to interpret $\Upsilon/\text{tr}[\hat{U}_{j,k}(t)]$ as a perturbation and invoke some topological stability argument; unfortunately $\Upsilon/\text{tr}[\hat{U}_{j,k}(t)]$ is neither bounded nor it is short-range. Moreover, one would like to have an explanation which distinguishes the situation in which $\hat{U}_{j,k}(t)$ is the product of two time-evolution according to topological and non-topological Hamiltonians. Intuitively, the argument must reside on the fact that any topological Hamiltonian spreads the localized zero-energy modes exponentially slower than non-topological Hamiltonians do.

In the Letter we present results also for thermal states. Because in this case the matrix $\hat{\rho}_{\pm}(t)$ is not a convex combination of a limited number of known pure states, we cannot exactly compute F_t^{opt} . Using the fact that $\hat{\rho}_{x,\pm} = \frac{1}{N_d} \sum_{j=1}^{N_d} e^{-i\hat{H}_j t} \hat{\rho}_{x,\pm}(0) e^{i\hat{H}_j t}$ and denoting $\hat{\rho}_{x,\pm}^{(j)} = e^{-i\hat{H}_j t} \hat{\rho}_{x,\pm}(0) e^{i\hat{H}_j t}$, we compute the following upper bound:

$$\begin{aligned} \|\hat{\rho}_{x,+} - \hat{\rho}_{x,-}\|_{\text{tr}} &\leq \min_{\pi \in S_{N_d}} \frac{1}{N_d} \sum_j^{N_d} \left\| \hat{\rho}_{x,+}^{(j)} - \hat{\rho}_{x,-}^{(\pi(j))} \right\|_{\text{tr}} \leq \\ &\leq \min_{\pi \in S_{N_d}} \frac{1}{N_d} \sum_j^{N_d} \sqrt{1 - F_U \left(\hat{\rho}_{x,+}^{(j)}, \hat{\rho}_{x,-}^{(\pi(j))} \right)^2} \end{aligned}$$

The minimization over the set of permutation of N_d elements can be done with the so-called ‘‘Hungarian algorithm’’ or ‘‘Kuhn-Munkres algorithm’’ [42]. The computation of the Uhlmann fidelity F_U between two mixed FGS has been explained in the section on FGS.

The fidelity of the optimal Gaussian operation requires the computation of the CM of $\hat{\rho}_{x,\pm}(t)$, which are not FGS. Because these states are convex combination of known FGS and because the CM is a linear function of the state, the CM of $\hat{\rho}_{x,\pm}(t)$ is:

$$\Gamma_{x,\pm} = \frac{1}{N_d} \sum_{j=1}^{N_d} \Gamma_{x,\pm}^{(j)} \quad (42)$$

where $\Gamma_{x,\pm}^{(j)}$ is the CM of $\hat{\rho}_{x,\pm}^{(j)}$.

* Electronic address: leonardo.mazza@sns.it

[1] M. Steger, K. Saeedi, M. L. W. Thewalt, J. J. L. Morton, H. Riemann, N. V. Abrosimov, P. Becker and H.-J. Pohl,

- Science **336**, 1280 (2012); P. C. Maurer, G. Kucsko, C. Latta, L. Jiang, N. Y. Yao, S. D. Bennett, F. Pastawski, D. Hunger, N. Chisholm, M. Markham, D. J. Twitchen, J. I. Cirac and M. D. Lukin, Science **336**, 1283 (2012).
- [2] N. Gisin and R. Thew, Nat. Phot. **1**, 165 (2007); T. D. Ladd, T. D. Ladd, F. Jelezko, R. Laflamme, Y. Nakamura, C. Monroe and J. L. O’Brien, Nature **464**, 45 (2010).
- [3] A. Y. Kitaev, arXiv:quant-ph/9707021v1, (1997).
- [4] E. Dennis, A. Y. Kitaev, A. Landahl, and J. Preskill, J. Math. Phys. **43**, 4452 (2002).
- [5] F. Pastawski, A. Kay, N Schuch and J. I. Cirac, Quantum Inf. Comput. **10**, 580 (2010).
- [6] M. A. Nielsen and I. L. Chuang, *Quantum Computation and Quantum Information*, Cambridge University Press (2000).
- [7] R. Alicki, M. Fannes and M. Horodecki, Jour. Phys. A **42**, 065303 (2009).
- [8] S. Bravyi and B. Terhal, New J. Phys. **11**, 043029 (2009).
- [9] S. Chesi, D. Loss, S. Bravyi and B. M. Terhal, New J. Phys. **12** 025013 (2010)
- [10] F. Pastawski, A. Kay, N Schuch and I. Cirac, Phys. Rev. Lett. **103**, 080501 (2009)
- [11] A. Kay, Phys. Rev. Lett. **107**, 270502 (2011)
- [12] S. Bravyi and R. König, Comm. in Math. Phys. **316**, 641 (2012).
- [13] S. Bravyi and J. Haah, arXiv:1112.3252 (2012)
- [14] A. Hutter, J. R. Wootton, B. Röthlisberger and D. Loss, arXiv:1206.0991 (2012)
- [15] M. Z. Hasan and C. L. Kane, Rev. Mod. Phys. **82**, 3045 (2010); X.-L. Qi and S.-C. Zhang, Rev. Mod. Phys. **83**, 1057 (2011).
- [16] N. Read and D. Green, Phys. Rev. B **61**, 10267 (2000).
- [17] A. Y. Kitaev, Physics-Uspekhi **44**, 131 (2001).
- [18] S. Bravyi, M. Hastings and S. Michalakis, J. Math. Phys. **51**, 093512 (2010).
- [19] J. C. Budich, S. Walter and B. Trauzettel, Phys. Rev. B **85**, 121405(R) (2012); D. Rainis and D. Loss, Phys. Rev. B **85**, 174533 (2012)
- [20] R. M. Lutchyn, J. D. Sau, and S. Das Sarma, Phys. Rev. Lett. **105**, 077001 (2010); Y. Oreg, G. Refael and F. von Oppen, Phys. Rev. Lett. **105**, 177002 (2010).
- [21] M. Sato, Y. Takahashi and S. Fujimoto, Phys. Rev. Lett. **103**, 020401 (2009); L. Jiang, T. Kitagawa, J. Alicea, A. R. Akhmerov, D. Pekker, G. Refael, J. I. Cirac, E. Demler, M. D. Lukin and P. Zoller, Phys. Rev. Lett. **106**, 220402 (2011); S. Diehl, E. Rico, M. A. Baranov and P. Zoller, Nat. Phys. **7**, 971 (2011).
- [22] V. Mourik, K. Zuo, S. M. Frolov, S. R. Plissard, E. P. A. M. Bakkers and L. P. Kouwenhoven, Science **336**, 1003 (2012).
- [23] G. Goldstein and C. Chamon, Phys Rev B **84**, 205109 (2011).
- [24] M. Cheng, R. M. Lutchyn and S. Das Sarma, Phys. Rev. B **85**, 165124 (2012); M. J. Schmidt, D. Rainis and D. Loss, Phys. Rev. B **86**, 085414 (2012).
- [25] A notable exception to such an assumption is Ref. [12], where it is shown that the addition of random perturbations leads to a sizable extension of the memory time in a scenario where other perturbations are present.
- [26] A. R. Akhmerov, Phys. Rev. B **82**, 020509 (2010).
- [27] D. Gottesman, Caltech Ph.D. thesis, arXiv:quant-ph/9705052 (1997).
- [28] A. Botero and B. Reznik, Phys. Lett. A **331**, 39 (2004);

- S. Bravyi, Quantum Info. Comput. **5**, 216 (2005).
- [29] Gaussian theories, consisting of operations and measurements which transform Gaussian states into Gaussian states, naturally appear in weakly interacting systems, and describe many experimental situations in a very natural fashion.
 - [30] Results would have been identical, apart from notation, in the odd sector $\text{span}\{|\tilde{0}\rangle = \hat{a}^\dagger|\text{vac}\rangle, |\tilde{1}\rangle = \hat{b}^\dagger|\text{vac}\rangle\}$
 - [31] If we denote by $\hat{\rho}(t)$ the state of the chains at time t , the map $\mathcal{D}_t : \hat{\rho}_q \rightarrow \hat{\rho}(t)$, where $\hat{\rho}_q$ is a qubit density operator characterized by $\langle \hat{\sigma}'_\alpha \rangle_{\hat{\rho}_q} = \langle \hat{\sigma}'_\alpha \rangle_{\hat{\rho}(0)}$, where the $\hat{\sigma}'$ are defined in (2).
 - [32] This is due to the contractivity of the trace norm [6].
 - [33] M. D. Bowdrey, D. K. L. Oi, A. J. Short, K. Banaszek and J. A. Jones, Phys. Lett. A **294**, 258 (2002).
 - [34] The effect of quartic terms, representing for instance interactions, will be analyzed in a forthcoming work using the methods developed in [35].
 - [35] C. Kraus and J.I. Cirac, New J. Phys **12** (2010), 113004
 - [36] J. R. Wootton and J. K. Pachos, Phys. Rev. Lett. **107**, 030503 (2011).
 - [37] C. Stark, L. Pollet, A. Imamoglu, and R. Renner, Phys. Rev. Lett. **107**, 030504 (2011).
 - [38] For any state, $\Gamma^T \Gamma \leq \mathbb{1}$ with equality only for pure Gaussian states. For any covariant matrix fulfilling this inequality, there exists a mixed Gaussian state corresponding to it.
 - [39] S. Bravyi and R. König, Quantum Inf. and Comp. **12**, 925 (2012); B. Horstmann, J. I. Cirac and G. Giedke, arXiv:1207.1653 (2012).
 - [40] C. Kraus and J.I. Cirac, New J. Phys **12** (2010), 113004
 - [41] B. M. Terhal and D. P. DiVincenzo, Phys. Rev. A **65** 032325 (2002).
 - [42] We use the implementation for Matlab written by Y. Cao which can be found at: <http://www.mathworks.com/matlabcentral/fileexchange/> with ID #20652 (2011).